Corrected 28 September 2022. See full text.

PHYSICAL CHEMISTRY

Proton-coupled energy transfer in molecular triads

Belinda Pettersson Rimgard[1]†, Zhen Tao[2]†‡, Giovanny A. Parada[2,3], Laura F. Cotter[2], Sharon Hammes-Schiffer[2]*, James M. Mayer[2]*, Leif Hammarström[1]*

We experimentally discovered and theoretically analyzed a photochemical mechanism, which we term proton-coupled energy transfer (PCEnT). A series of anthracene-phenol-pyridine triads formed a local excited anthracene state after light excitation at a wavelength of ~400 nanometers (nm), which led to fluorescence around 550 nm from the phenol-pyridine unit. Direct excitation of phenol-pyridine would have required ~330-nm light, but the coupled proton transfer within the phenol-pyridine unit lowered its excited-state energy so that it could accept excitation energy from anthracene. Singlet-singlet energy transfer thus occurred despite the lack of spectral overlap between the anthracene fluorescence and the phenol-pyridine absorption. Moreover, theoretical calculations indicated negligible charge transfer between the anthracene and phenol-pyridine units. We construe PCEnT as an elementary reaction of possible relevance to biological systems and future photonic devices.

Coupling of proton transfer to electronic transitions exerts a great influence on the energetics and kinetics of these processes. Photoacids are well-studied examples, where light excitation leads to a rapid proton release and, in some cases, even produces long-lived pH changes and pH gradients (*1*, *2*). Another example is excited-state intramolecular proton transfer (ESIPT), which generates an excited tautomer state of the light-absorbing molecule; systems where this state is fluorescent have applications for optoelectronic materials (*3*). Often, ESIPT instead allows for ultrafast dissipation of excess electronic energy as heat, and is therefore an important photostabilizing mechanism in plastics (*4*) as well as in biomolecules such as DNA (*5*).

More recently, the charge transfer mechanism of proton-coupled electron transfer (PCET) has generated great interest (*6*). PCET is a key reaction behind biological energy conversion in photosynthesis, respiration, and nitrogen fixation (*7*), as well as in synthetic chemical systems for photoredox catalysis and renewable energy conversion and storage (*8*–*11*). It is also involved in DNA synthesis and repair, photoreceptor function, and many other radical enzyme reactions (*12*–*15*). Of particular interest is the concerted PCET mechanism, where the electron and proton are transferred without the formation of high-energy intermediates, thereby offering a low-barrier reaction pathway.

[1]Department of Chemistry - Ångström Laboratory, Uppsala University, SE 75120 Uppsala, Sweden. [2]Department of Chemistry, Yale University, New Haven, CT 06520, USA. [3]Department of Chemistry, College of New Jersey, Ewing, NJ 08628, USA.
†These authors contributed equally to this work. ‡Present address: Department of Chemistry, University of Pennsylvania, Philadelphia, PA 19104, USA.
*Corresponding author. Email: sharon.hammes-schiffer@yale.edu (S.H.-S.); james.mayer@yale.edu (J.M.M.); leif.hammarstrom@kemi.uu.se (L.H.)

In all the above reactions, the coupled transfer of the proton changes the energy landscape of the overall process, which obviously affects its dynamics and rate. There are also important effects of the much greater mass of the proton, whose wave function is more localized than that of the electrons involved, which may impose a greater sense of directionality on the process. Understanding and analyzing such effects, theoretically and experimentally, is a fundamentally interesting challenge and of practical importance.

In 2019, our groups used a series of anthracene-phenol-pyridine (An-PhOH-Py) triads (Fig. 1) (*16*) to demonstrate the first example of concerted PCET occurring in the Marcus inverted region (*17*). This behavior, where the rate decreases with increasing driving force, is important for slowing recombination after photochemical charge separation, but was previously considered unlikely for concerted PCET reactions because of the nearly barrierless tunneling to higher vibrational product states (*18*). Nonetheless, photoexcitation of the An subunit of the triads results in the formation of a local excited state (LES) on the anthracene (Eq. 1) (*16*, *19*). In tenths of picoseconds, the LES forms the charge-separated state (CSS) by electron transfer from the PhOH group to the ^{1}*An concerted with proton transfer to the pyridine

	R_1	R_2
1	CN	4-Me
2	CN	4-OMe
3	CN	4-NMe_2
4	CN	4-CN
5	H	4-Me
6	H	H
7	H	4-CF_3
8	H	6-CF_3

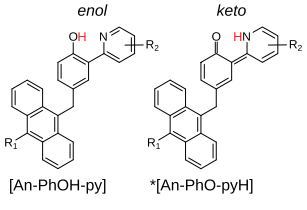

Fig. 1. Structures of the studied anthracene-phenol-pyridine ([An-PhOH-py]) triads. The enol form is the stable ground-state form, and the electronically excited keto form is the local electron-proton transfer (LEPT) state.

(Eq. 2). The charges subsequently recombine to the ground-state reactants (Eq. 3), once again in a concerted electron-proton transfer reaction but with a large driving force (>2.0 eV in CH_3CN). This process consequently places the reaction in the inverted region, as was shown by the rate dependence on driving force and solvent polarity.

$$\text{An-PhOH-py} \xrightarrow{h\nu} {}^1\text{*An-PhOH-py(LES)} \quad (1)$$

$${}^1\text{*An-PhOH-py} \rightarrow \text{An}^{\bullet-}\text{-PhO}^{\bullet}\text{-pyH}^{+}\text{(CSS)} \quad (2)$$

$$\text{An}^{\bullet-}\text{-PhO}^{\bullet}\text{-pyH}^{+} \rightarrow \text{An-PhOH-py} \quad (3)$$

The CSS intermediate was observed only in triads **1** to **3**, however; in triads **4** to **8**, a similar quenching of the LES did not result in an observable CSS (*16*). This result is puzzling, as the charge recombination driving force is larger for **4** to **8**, meaning the reaction would be more deeply in the inverted region and thus even slower than for **1** to **3**. Theoretical investigations have suggested the involvement of another state that would lie lower than the CSS in **4** to **8** (*20*, *21*). This is the so-called local electron-proton transfer (LEPT) state, where the PhOH-py fragment is in a local, electronically excited tautomeric (keto) state, *[PhO-pyH], in which the phenolic proton has transferred to the pyridine. The LEPT state is the same excited tautomeric state as that formed by ESIPT after excitation of the separate phenol-pyridine compound (*22*), and similar to other ESIPT compounds (*3*). This state was proposed to be populated after excitation in **4** to **8** (*20*, *21*); it can possibly be populated from the CSS (Eq. 4) or be formed directly from the LES (Eq. 5) by a process here denoted proton-coupled energy transfer, PCEnT (see below).

$$\text{An}^{\bullet-}\text{-PhO}^{\bullet}\text{-pyH}^{+} \rightarrow \text{An-}{}^*[\text{PhO-pyH}]\text{(LEPT)} \quad (4)$$

$${}^1\text{*An-PhOH-py} \xrightarrow{\text{PCEnT}} \text{An-}{}^*[\text{PhO-pyH}]\text{(LEPT)} \quad (5)$$

Here, we present experimental and theoretical evidence for direct formation of the fluorescent LEPT state from the LES at 77 K in a butyronitrile glass, in which formation of the CSS is inhibited. In this experimental example of PCEnT, excitation energy was transferred from ^{1}*An to ^{1}*[PhO-pyH], coupled to proton transfer within the PhOH-py unit (Eq. 5). This finding was surprising, as it is a singlet-singlet transition without any detectable spectral overlap between the donor fluorescence and acceptor absorption. Moreover, PCEnT occurred with negligible charge transfer between the An and PhOH-py units, which is in sharp contrast to PCET reactions. This result significantly expands the scope of concerted processes where

Corrected 30 September 2022. See full text.

proton transfer controls reactivity. Many excited-state charge and energy transfer reactions in proteins and DNA occur between hydrogen-bonded pigments, making PCEnT possibly important in natural systems. Yet such a reaction has, to the best of our knowledge, not previously been reported.

Spectroscopic observation of LEPT state

The lack of observed CSS formation in triads **4** to **8**, together with the computationally predicted excited-state keto tautomer (LEPT) (*20*), laid the basis for further investigation. The triad absorption spectra agree well with a sum of contributions from the separate components: a vibrationally structured anthracene band around 400 nm and a PhOH-py band around 330 nm (Fig. 2B and fig. S1). The LEPT state should fluoresce around 500 nm in aprotic, rigid media, as has been shown for the excited keto state, *[PhO-pyH] of the separate phenol-pyridine compound (*22*). Therefore, we examined the triads (**1**, **2**, **4** to **7**) by fluorescence spectroscopy in rigid butyronitrile glass at T = 77 K. We also studied these triads computationally and found that the minimum-energy LEPT geometry exhibits a ~90° twist between the phenol and pyridine fragments, whereas the planar LEPT geometry is a first-order saddle point. This twisting, which is known to quench the fluorescence (*22*, *23*), is expected to be hindered in the glass at 77 K. Thus, the computational studies were performed for both the planar and twisted LEPT geometries.

The 77 K fluorescence spectrum of **1**, after selective excitation of the An unit at 400 nm, showed a structured ^{1}*An fluorescence at 420 to 580 nm, accompanied by a broad band with a maximum around 550 nm (Fig. 2B). The latter is expected for the LEPT state (*22*) and was similarly observed for all measured triads with an electron-donating group on the pyridine: **1**, **2**, **5**, and **6** (Fig. 2, B and C). The LEPT emission shifted to lower energy when the electron-donating group was weaker (**2** > **1** > **6**), consistent with the computational results in tables S8 and S12. Because **1** and **5** share the same functional group (R_2 = 4-Me) on the pyridine, the LEPT energy should be similar. Still, the peak for **5** was blueshifted by 11 nm, which indicated a small but significant coupling to the An unit, which differs in its functional group (CN in **1**; H in **5**) between these triads. The relative intensity of the ^{1}*An and LEPT fluorescence was independent of triad concentration (fig. S2), and control experiments with 9-CN-10-Me-An showed only the structured ^{1}*An fluorescence (Fig. 2B). This excluded any excimer or other anthracene complex as responsible for the broad fluorescence around 550 nm.

Fluorescence excitation spectroscopy provided unambiguous evidence for LEPT state formation from excited ^{1}*An (Fig. 2D). The shape of the excitation spectrum of the 550-nm LEPT emission peak (purple line) matched that of the absorption spectrum (black line), with contributions from both the PhOH-py (330 nm) and the An (300 to 430 nm) absorption bands. The excitation spectrum of the 450-nm ^{1}*An emission (green line) showed instead a weaker relative contribution from the 330-nm PhOH-py band. The 550-nm LEPT state could thus be formed either by exciting the PhOH-py unit, which would cause formation of the LEPT state by the well-established ESIPT mechanism, or directly via excitation of the An unit followed by energy transfer from ^{1}*An.

Evidence for proton-coupled energy transfer mechanism

The excitation energy transfer from the anthracene donor to the phenol-pyridine unit to yield the LEPT state is a type of mechanism that we denote proton-coupled energy transfer, PCEnT (Fig. 2A). Energy transfer directly to the *[PhOH-py] state would be strongly uphill, as is seen from its low-wavelength absorption spectrum around 330 nm, but proton

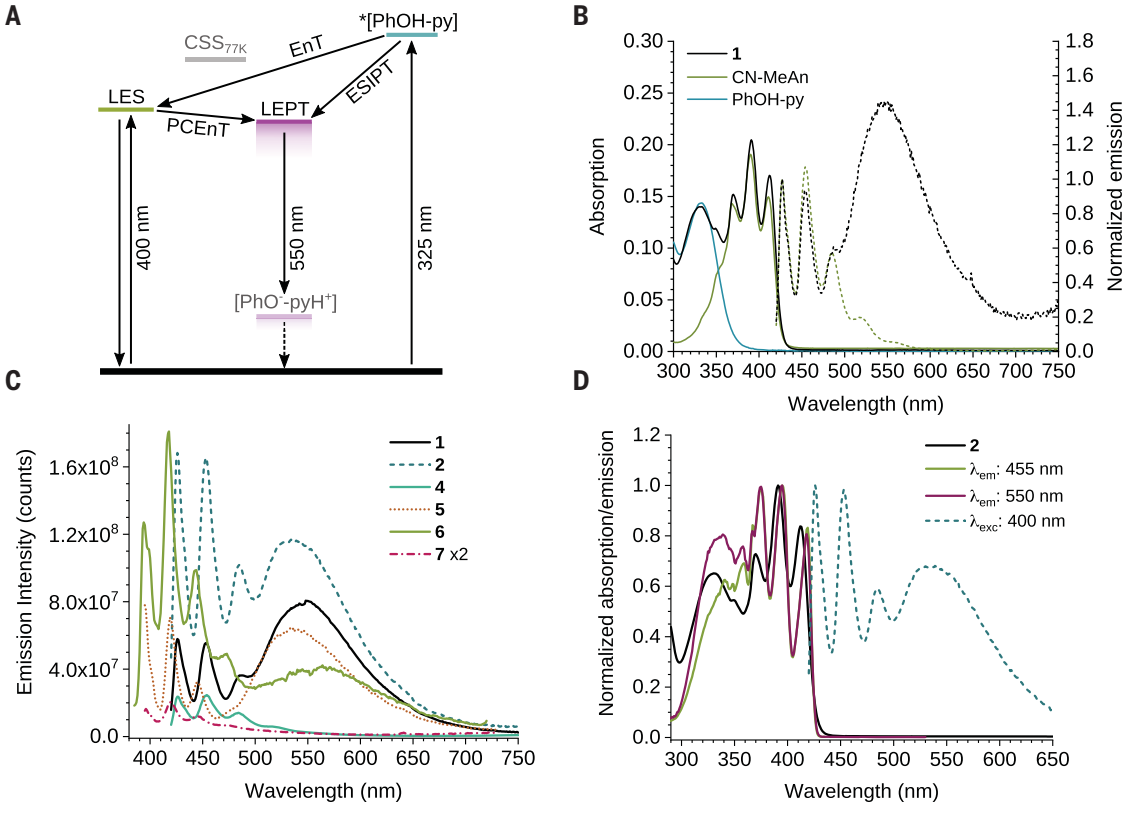

Fig. 2. Steady-state absorption (room temperature) and fluorescence (77 K) spectra in butyronitrile. (**A**) Schematic Jablonski diagram of the possible transitions at 77 K for the triads: radiative decay (downward solid line) and nonradiative decay. The CSS energy depends strongly on the chemical environment (*16*, *19*) and is higher than the LES at 77 K. (**B**) Absorption (solid line) and fluorescence spectra normalized to the first An emission peak (dashed line, λ_{exc}: 400 nm) of **1** (black) and the reference compounds of similar concentrations (4 to 7 μM): 2,4-di-*tert*-butyl-6-(pyridin-2-yl)phenol (PhOH-py, blue) and 9-cyano-10-methylanthracene (CN-MeAn, green). (**C**) Fluorescence spectra of triads **1**, **2**, **4**, **5**, **6**, and **7** with excitation at 400 nm (**1** and **2**), 365 nm (**6**), and 375 nm (**5** and **7**). Note that **7** was measured with twice the absorption at the excitation wavelength. (**D**) Absorption spectrum (black line), fluorescence excitation spectrum (λ_{em} = 455 and 550 nm, solid line) and fluorescence spectrum (λ_{exc} = 400 nm, dashed line) of **2**.

Corrected 30 September 2022. See full text.

transfer lowers the phenol-pyridine excited-state energy to make the PCEnT process energetically feasible. The quantum yield for the LEPT formation was deemed to be similar irrespective of which fragment was excited, on the basis of the good agreement between the shapes of the absorption spectrum (Fig. 2D) and the 550-nm excitation spectrum, where the respective PhOH-py and An amplitudes were fairly equal in the two spectra. This fact shows that PCEnT from ^{1}*An was about as efficient as ESIPT from *[PhOH-py].

To follow the formation and decay of the LEPT state in real time, we performed ultrafast transient fluorescence spectroscopy measurements of **6** with excitation at 370 nm, in the mid- to red part of the An absorption band (Fig. 3). The observed features matched those seen in the steady-state experiments, and global fits were performed within the peak regions of the LES (380 to 490 nm) and LEPT (520 to 655 nm) fluorescence (Fig. 3B). The rise time of the LEPT peak was fitted to ~44 ps and a similarly short decay component could be found for the LES (46 ps), which reinforced the notion that the LEPT state could be populated directly from the LES (as depicted in the overall reaction scheme in Fig. 2A).

We can exclude LEPT formation via a sequential LES-CSS-LEPT reaction at 77 K, because the CSS would be substantially destabilized in a solvent glass (Fig. 2A) as a result of its greater dipole moment relative to both the LES and LEPT (Fig. 4B). Moreover, the solvent glass at 77 K prevented the large degree of twisting of the An group to reach the CSS optimized structure (Fig. 4B and table S1), which further destabilized the CSS energy. The CSS lies less than 0.2 eV below the LES at room temperature (*16*), and small-molecule charge separation is typically destabilized by more than 0.5 eV by freezing out solvent repolarization

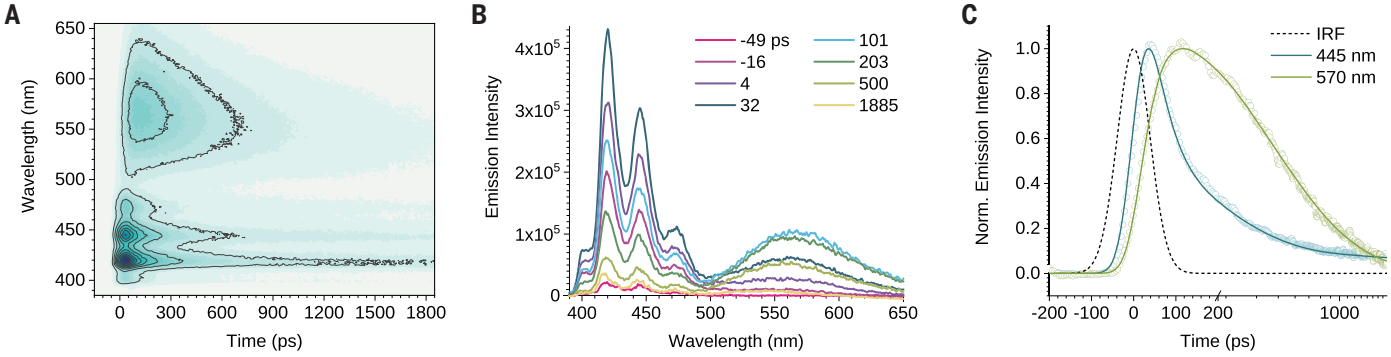

Fig. 3. Transient fluorescence emission spectra in butyronitrile at 77 K. (**A**) Contour map of the transient fluorescence emission intensity counts (dark blue = highest intensity) of **6** in butyronitrile (0.2 mM) between 390 and 640 nm within a 2-ns time window. (**B**) Emission spectra at given times after excitation with 370-nm light. The ^{1}*An fluorescence reaches a maximum at ~30 ps (instrumental response function IRF_{FWHM} = 65 ps) and decreases simultaneously with the the rise of LEPT fluorescence that maximizes after ~140 ps. (**C**) Time-resolved fluorescence traces (lines, fit; circles, data) within the LES (445 nm, blue line) and LEPT (570 nm, green line) bands; the IRF is shown as a dashed line.

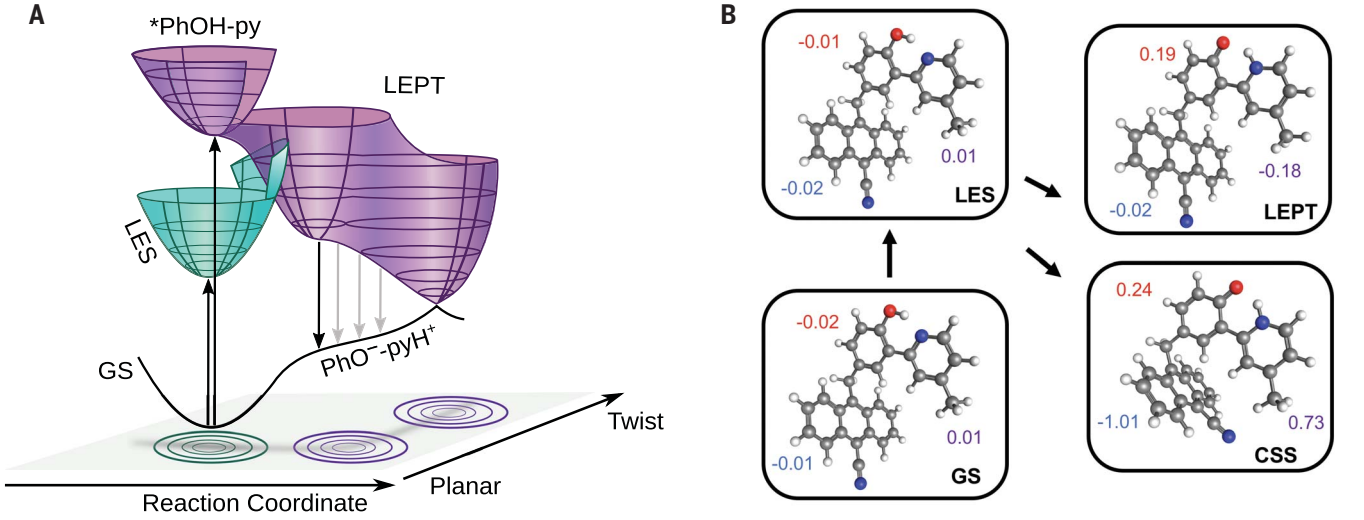

Fig. 4. Potential energy surfaces and optimized structures for the electronic states discussed. (**A**) Schematic potential energy surfaces for the ESIPT and PCEnT reactions, color-coded to mark the electronically excited fragment (green, An; purple, PhOH-py). Note that ESIPT is barrierless on the excited-state potential energy surface (purple), whereas PCEnT follows the reorganization of the heavy nuclei including the solvent (green to purple). In fluid solution, the LEPT state will twist along the PhOH-py bond, where 90° leads to a conical intersection, and nonradiative decay. This twist is impeded in the 77 K butyronitrile glass, although a partial twist could occur to lower the energy of the LEPT state relative to the LES (table S11). GS, ground state. (**B**) The optimized structures and the natural bond orbital [NBO (*31*)] charges on the anthracene (blue), phenol (red), and pyridine (purple) subunits of **1** for the GS, LES, CSS, and planar (not twisted, first-order saddle point) LEPT state in the gas phase. The charges reflect the electron density, where a more negative number equals a more electron-dense fragment (the methylene spacer between anthracene and phenol is not included in any of the fragments, and therefore those charges are excluded in this analysis).

Corrected 30 September 2022. See full text.

in polar solvents (*24*). Our gas-phase calculations in table S6 indeed placed the CSS higher than the LES. Moreover, the LEPT fluorescence was formed faster in **6** (~44 ps) than in **1** (~69 ps), despite greater room-temperature driving force for CSS formation (by ~0.5 eV) in the latter (*16*); this is clear experimental proof against a reaction involving the CSS.

The photophysics of triads **1** to **8** have been previously studied by transient absorption (TA) at ambient temperature (*16*), and **6** was also examined by time-resolved fluorescence spectroscopy at various temperatures (*25*). In the TA study at room temperature, the initial anthracene LESs in **1** to **3** decayed to a long-lived state (up to τ = 755 ps) with spectral features in agreement with the CSS being formed by PCET, including obvious features of the anthracene anion. The same mechanism was assigned to the decay of the LES of **4** to **8** on the basis of the close correlation of LES decay rates with the free energies of PCET for each triad. These triads did not show a long-lived transient in the TA spectra at ambient temperatures. However, computations later placed the LEPT state below the CSS for **4** and **6** (*20*), indicating that rapid CSS-to-LEPT conversion and/or a contribution of PCEnT from the LES would be reasonable.

The previously reported spectrally resolved ultrafast fluorescence spectra of **6** at ambient temperatures showed an H/D kinetic isotope effect (KIE) = 4 and did not show any evidence of emission from a LEPT state. At lower temperatures, in a 2-methyl-tetrahydrofuran (2-Me-THF) glass or a polymethylmethacrylate (PMMA) film, the subnanosecond integrated fluorescence followed a single exponential with $\tau \approx 150$ ps, with an unexplained long–time scale ($\gg$ ns) component. The data in 2-Me-THF were obtained in the presence of 3% methanol, which was observed to quench the LEPT emission in the current study. Therefore, the two studies are not directly comparable. In retrospect, these data could be consistent with the LES decaying either by PCET or by the new PCEnT pathway reported here in butyronitrile glasses; additional studies are needed.

Physical principles underlying proton-coupled energy transfer

The observation that PCEnT directly formed the excited tautomeric LEPT state was surprising and needs mechanistic clarification. As both the ^{1}*An and the LEPT state are fluorescent, PCEnT is clearly a singlet-singlet process. However, there was no detectable spectral overlap between the donor fluorescence and acceptor ground-state absorption (Fig. 2B), which is a requirement for Förster (dipole-dipole) energy transfer. The absence of low-energy absorption of the keto form [PhO^--pyH^+] is because the ground state, at the LEPT geometry, lies ~0.5 eV higher than the enolic ground state (table S4) and was thus not populated to any appreciable extent. Instead, as the reaction occurred at quite a small donor-acceptor distance (~6 Å between the central rings of An and PhOH), the coupling was presumably dominated by exchange and/or penetration terms (*26*). Any stronger coupling mechanism was probably prevented by the methylene spacer between the subunits.

We propose, therefore, that PCEnT could be described by a nonadiabatic surface crossing (Fig. 4A), in analogy to Marcus-type theoretical descriptions of PCET (*6*, *7*). Thermal fluctuations of heavy nuclei lead to a configuration where electronic energy transfer and proton tunneling occur with energy conservation (crossing point of the reactant and product free energy curves). It is different from PCET, however, in that there is no charge transfer between donor and acceptor. The product state is a fluorescent excited state when phenol-pyridine twisting is hindered, and can thus be readily detected. Moreover, this mechanism differs from an ESIPT reaction, where proton transfer is driven by intramolecular charge redistribution, and the electronic coupling is usually strong, which leads to ultrafast reactions. The PCEnT reaction described here was instead driven by a remote, weakly coupled electronically excited state. The term "proton-coupled energy transfer" was previously used for two other types of processes, in which energy transfer was proposed to be modulated by either a hydrogen bond (*27*) or a reagent protonation state (*28*). By contrast, the proton is transferred during the PCEnT process studied in the present work and affects the energetics and dynamics in a critical manner.

The rearrangement from the enol to the keto form of the phenol-pyridine acceptor unit is much greater than just the transfer of a proton, as it involves substantial charge redistribution and changes in bond lengths and angles. These

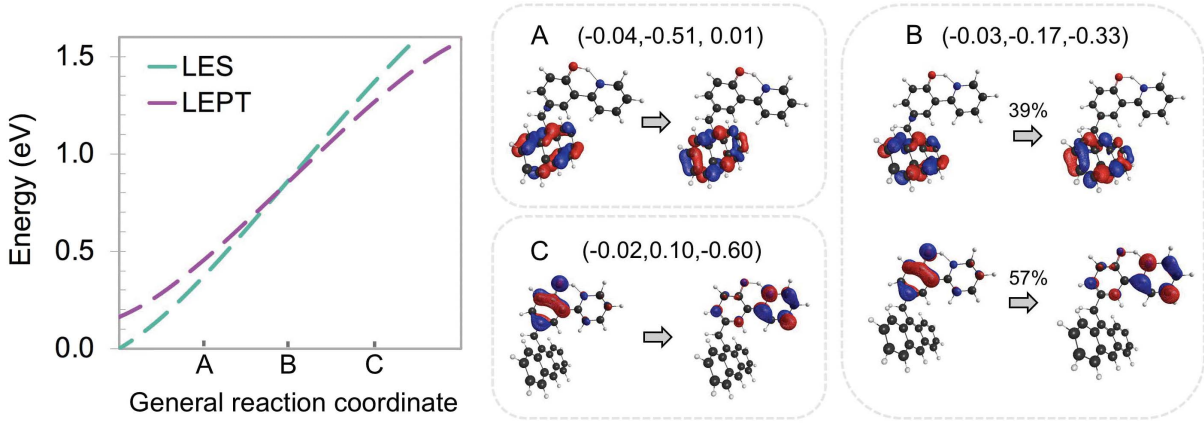

Fig. 5. Avoided-crossing region between the S_1 and S_2 adiabatic electronic states for triad 6, corresponding to a crossing between the LES and LEPT diabatic electronic states, and analysis of the S_1 excited state for relevant configurations. The energy curves were obtained from an excited-state adiabatic molecular dynamics trajectory and are plotted along a unitless general reaction coordinate rather than time; this trajectory is far from equilibrium and is not directly comparable to experiment because of the reaction conditions (supplementary text). (**A** to **C**) Configurations obtained from this trajectory. The dominant natural transition orbitals (NTOs), corresponding to the transitions from occupied to virtual orbitals that characterize the S_1 excited state, are shown for these three configurations. For (A), the NTOs are localized on the anthracene (LES), whereas for (C), the NTOs are localized on the phenol-pyridine fragment (LEPT state), where the proton has mostly transferred. For (B), an approximately equal mixture of LES and LEPT is observed, as indicated by the two NTOs. Above the orbital drawings of each configuration, the numbers are the charges (in a.u., the elementary charge of an electron) of the anthracene, phenol, and pyridine fragments for the S_1 state, in that order (excluding the charge of the CH_2 bridging group and the transferring hydrogen, which has a charge of ~0.5 a.u.).

Corrected 30 September 2022. See full text.

combined effects change the excitation energy of the phenol-pyridine acceptor unit and allow it to come into resonance with that of the anthracene. This behavior is the fundamental basis for coupling of proton transfer to energy transfer and distinguishes PCEnT from typical energy transfer reactions. The details of this coupling and the role of coupling with different proton vibrational states remain to be further explored.

Figure 5 demonstrates the PCEnT process observed in a molecular dynamics trajectory for triad **6** propagated on the S_1 state, which changed from LES to LEPT character as the proton transferred from the phenol to the pyridine. Representative configurations along this trajectory, along with an analysis of the fragment charges and dominant natural transition orbitals, show that the character of the S_1 state changed from LES to a mixture of LES and LEPT and then to LEPT. The nonadiabatic coupling between the S_1 and S_2 adiabatic electronic states (*29*, *30*) exhibited a peak at the avoided crossing, providing evidence that this process is nonadiabatic. Throughout this process, the charge on the anthracene fragment remained virtually zero, indicating that the LES-to-LEPT transition did not involve charge transfer between anthracene and the phenol-pyridine group, consistent with the PCEnT mechanism. Moreover, the net charge transfer from the phenol to the pyridine was also nearly zero after accounting for the charge of the transferring proton. In the framework of the vibronically nonadiabatic PCET theory (*6*), the transferring proton would be treated quantum mechanically and would tunnel during the LES-to-LEPT transition.

Conclusions and outlook

We have experimentally proved the involvement of the excited *[PhO-pyH] (LEPT) state, in the photochemical reactions of these triad molecules. This mechanism competes with PCET from the LES and could explain why the CSS was not observed in **4** to **8**. The LEPT state was formed by a novel proton-coupled energy transfer (PCEnT) mechanism. This is a singlet-singlet exchange energy transfer, coupled to proton transfer in the acceptor unit, that can be described as a nonadiabatic transition to the excited product state. Its free energy barrier in turn is determined by the reorganization energy associated with the solvent and other heavy nuclei, similar to Marcus ET theory or PCET theories (*6*, *17*). In contrast to PCET, there is negligible charge transfer between donor and acceptor.

This mechanism can have several intriguing implications for both natural and synthetic systems. PCEnT may allow for the photosensitization of otherwise dark states, such as seen here by the LEPT formation from the low energy excitation of the LES, rather than the direct excitation of the PhOH-py unit at higher energy (ca 330 nm). Moreover, as energy transfer occurs over long distances but proton transfer is short-range, we suggest that this mechanism may be of importance to direct energy migration in e.g., light-harvesting systems and photonic materials, where the PCEnT acceptor would form a low-energy site. PCEnT could also form the basis of a molecular switch for energy transfer, where proton transfer could be controlled independently by hydrogen-bonding or (de)protonation, thus effectively turning energy transfer on or off. We speculate that these processes could already be operational in natural systems with hydrogen-bonded light-absorbers, such as porphyrins in photosynthetic assemblies, DNA and flavin proteins, but have yet to be identified.

REFERENCES AND NOTES

1. Y. Liao, *Acc. Chem. Res.* **50**, 1956–1964 (2017).
2. L. Schulte, W. White, L. A. Renna, S. Ardo, *Joule* **5**, 2380–2394 (2021).
3. A. P. Demchenko, K.-C. Tang, P.-T. Chou, *Chem. Soc. Rev.* **42**, 1379–1408 (2013).
4. J. Catalan *et al*., *J. Am. Chem. Soc.* **114**, 5039–5048 (1992).
5. A. L. Sobolewski, W. Domcke, C. Hättig, *Proc. Natl. Acad. Sci. U.S.A.* **102**, 17903–17906 (2005).
6. S. Hammes-Schiffer, A. A. Stuchebrukhov, *Chem. Rev.* **110**, 6939–6960 (2010).
7. A. Migliore, N. F. Polizzi, M. J. Therien, D. N. Beratan, *Chem. Rev.* **114**, 3381–3465 (2014).
8. J. J. Warren, T. A. Tronic, J. M. Mayer, *Chem. Rev.* **110**, 6961–7001 (2010).
9. P. R. D. Murray *et al*., *Chem. Rev.* **122**, 2017–2291 (2022).
10. N. S. Lewis, D. G. Nocera, *Proc. Natl. Acad. Sci. U.S.A.* **103**, 15729–15735 (2006).
11. R. Tyburski, T. Liu, S. D. Glover, L. Hammarström, *J. Am. Chem. Soc.* **143**, 560–576 (2021).
12. J. Stubbe, D. G. Nocera, C. S. Yee, M. C. Y. Chang, *Chem. Rev.* **103**, 2167–2201 (2003).
13. C. Aubert, M. H. Vos, P. Mathis, A. P. M. Eker, K. Brettel, *Nature* **405**, 586–590 (2000).
14. F. Lacombat *et al*., *J. Am. Chem. Soc.* **141**, 13394–13409 (2019).
15. S. Hu, A. V. Soudackov, S. Hammes-Schiffer, J. P. Klinman, *ACS Catal.* **7**, 3569–3574 (2017).
16. G. A. Parada *et al*., *Science* **364**, 471–475 (2019).
17. R. Marcus, N. Sutin, *Biochim. Biophys. Acta Rev. Bioenerg.* **811**, 265–322 (1985).
18. S. J. Edwards, A. V. Soudackov, S. Hammes-Schiffer, *J. Phys. Chem. B* **113**, 14545–14548 (2009).
19. L. F. Cotter, B. Pettersson Rimgard, G. A. Parada, J. M. Mayer, L. Hammarström, *J. Phys. Chem. A* **125**, 7670–7684 (2021).
20. E. R. Sayfutyarova, S. Hammes-Schiffer, *J. Am. Chem. Soc.* **142**, 487–494 (2020).
21. E. R. Sayfutyarova, S. Hammes-Schiffer, *J. Phys. Chem. Lett.* **11**, 7109–7115 (2020).
22. D. LeGourriérec, V. Kharlanov, R. G. Brown, W. Rettig, *J. Photochem. Photobiol. Chem.* **117**, 209–216 (1998).
23. S. Kim, J. Seo, S. Y. Park, *J. Photochem. Photobiol. Chem.* **191**, 19–24 (2007).
24. G. L. GainesIII, M. P. O'Neil, W. A. Svec, M. P. Niemczyk, M. R. Wasielewski, *J. Am. Chem. Soc.* **113**, 719–721 (1991).
25. M. A. Bowring *et al*., *J. Am. Chem. Soc.* **140**, 7449–7452 (2018).
26. G. D. Scholes, K. P. Ghiggino, *J. Phys. Chem.* **98**, 4580–4590 (1994).
27. E. R. Young, J. Rosenthal, D. G. Nocera, *Chem. Sci.* **3**, 455–459 (2012).
28. C. Drolen *et al*., *J. Am. Chem. Soc.* **140**, 10169–10178 (2018).
29. S. Fatehi, E. Alguire, Y. Shao, J. E. Subotnik, *J. Chem. Phys.* **135**, 234105–234121 (2011).
30. Q. Ou, G. D. Bellchambers, F. Furche, J. E. Subotnik, *J. Chem. Phys.* **142**, 064114–14 (2015).
31. A. E. Reed, L. A. Curtiss, F. Weinhold, *Chem. Rev.* **88**, 899–926 (1988).
32. B. Pettersson Rimgard *et al*., Data for "Proton-coupled energy transfer in molecular triads," Open Science Framework. DOI: 10.17605/OSF.IO/JY46X.

ACKNOWLEDGMENTS

We acknowledge N. Kaul, L. D'Amario, and E. Sayfutyarova for their expertise and helpful discussions. **Funding:** Supported by Swedish Research Council grant 2020-05246 and NIH grants 2R01GM50422, R35GM144105-01, and R35GM139449. **Author contributions:** B.P.R. and L.H. conceived the project and, together with Z.T. and S.H.-S., they wrote the paper. B.P.R., L.F.C., and G.A.P. collected the data, and B.P.R. analyzed all the data. Z.T. and S.H.S. performed all the computational work. All authors participated in active discussions and reviewed the manuscript. **Competing interests:** The authors have no competing interests. **Data and materials availability:** All data needed to evaluate the conclusions in the paper are present in the paper or the supplementary materials. An Excel file with steady-state and time-resolved absorption and fluorescence data, as well as the optimized geometry for triads **1** and **6**, and their NBO charges, has been deposited in the Open Science Framework (*32*).

SUPPLEMENTARY MATERIALS

science.org/doi/10.1126/science.abq5173
Materials and Methods
Supplementary Text
Figs. S1 to S11
Tables S1 to S13
References (*33*–*52*)
Data S1

Submitted 13 April 2022; accepted 7 July 2022
Published online 21 July 2022
10.1126/science.abq5173